HHS Public Access

Author manuscript

J Invest Dermatol. Author manuscript; available in PMC 2016 April 01.

Published in final edited form as:

J Invest Dermatol. 2015 October ; 135(10): 2519–2529. doi:10.1038/jid.2015.182.

Acellular hydrogel for regenerative burn wound healing: translation from a porcine model

Yu-I Shen[#1], **Hyun-Ho Greco Song**[#1], **Arianne Papa**[2], **Jacqueline Burke**[2], **Susan W Volk**[3], and **Sharon Gerecht**[1,4,§]

[1] Department of Chemical and Biomolecular Engineering, Johns Hopkins Physical Sciences - Oncology Center and Institute for NanoBioTechnology, Johns Hopkins University, 3400 North Charles street, Baltimore, MD 21218, USA

[2] Department of Biomedical Engineering, Johns Hopkins University, 3400 North Charles street, Baltimore, MD 21218, USA

[3] Department of Clinical Studies--Philadelphia, University of Pennsylvania School of Veterinary Medicine, 380 S. University Ave, Philadelphia, PA 19104, USA

[4] Department of Materials Science and Engineering, Johns Hopkins University, 3400 North Charles street, Baltimore, MD 21218, USA

[#] These authors contributed equally to this work.

Abstract

Currently available skin grafts and skin substitute for healing following third-degree burn injuries is fraught with complications, often resulting in long-term physical and psychological sequelae. Synthetic treatment that can promote wound healing in a regenerative fashion would provide an off-the-shelf, non-immunogenic strategy to improve clinical care of severe burn wounds. Here, we demonstrate vulnerary efficacy and accelerated healing mechanism of dextran-based hydrogel in third-degree porcine burn model. The model was optimized to allow examination of the hydrogel treatment for clinical translation and its regenerative response mechanisms. Hydrogel treatment accelerated third-degree burn wound healing by rapid wound closure, improved reepithelialization, enhanced extracellular matrix remodeling, and greater nerve reinnervation, compared to the dressing treated group. These effects appear to be mediated through the ability of the hydrogel to facilitate a rapid but brief initial inflammatory response that coherently stimulates

[§]Corresponding *author: gerecht@jhu.edu*.

Author contributions: Y-I.S., and H-H.G.S: Designed and performed research, analyzed data, and wrote the paper; **A.P and J.B:** analyzed data; **S.W.V:** Analyzed data and wrote the paper; **S.G:** Designed research, analyzed data, and wrote the paper.

Conflict of Interest: Intellectual property related to the hydrogel technology is owned by Johns Hopkins University and licensed to Gemstone Biotherapeutics LLC of which S.G. is a cofounder, consultant, and director. S.G has a financial interest in Gemstone Biotherapeutics LLC, which is subject to certain restrictions under University policy. The terms of this arrangement are being managed by the Johns Hopkins University in accordance with its conflict of interest policies. S.W.V received fees for service consulting for Gemstone Biotherapeutics LLC. Gemstone Biotherapeutics LLC did not affect the design, interpretation, or reporting of any of the experiments herein. Y-I. S., H-H.G.S., A.P. and J.B. report that they have no competing interests. **Data and materials availability:** Hydrogel technology described here can be synthesized from commercially available materials as described in Materials and Methods. Depending on availability, hydrogels can be transferred upon request to other academic researchers using letter agreements that conform to the intent of the Material Transfer Agreement (MTA).

neovascularization within the granulation tissue during the first week of treatment, followed by an efficient vascular regression to promote a regenerative healing process. Our results suggest that the dextran-based hydrogels may substantially improve healing quality and reduce skin grafting incidents and thus pave the way for clinical studies to improve the care of severe burn injury patients.

Introduction

In 2013, approximately 450,000 burn injuries received medical treatment (Stoddard *et al.*, 2014) and the estimated hospital care cost in high-income countries estimated to exceed $88,000 per burn patient (Hop *et al.*, 2014). Survival in the most severely burned patients is often accompanied with orthopedic, neurologic and metabolic complications and significant psychosocial challenges brought about by poor healing and excessive scar formation (Stoddard *et al.*, 2014). Therefore, challenges remain to improve serious burns wound healing. . Unlike superficial burn wounds that can heal on their own without advanced professional care, third-degree burn, which are characterized by the full-thickness damage of the skin, most often require surgical intervention and replacement of damaged skin with skin grafts or skin substitutes (Sheridan, 2012). Biomaterials that are able to induce a regenerative response of healing would therefore promise significant improvement in clinical care and long-term outcomes of wound patients, particularly those sustaining burn injury.

Porcine wound healing is considered to be most similar to that of humans and as a translational model, pigs display the greatest concordance with human trials (Sullivan *et al.*, 2001). First, porcine skin most closely resembles human skin both anatomically and physiologically. Both have similar dermal-epidermal thickness ratio and dermal vascularization pattern (Middelkoop *et al.*, 2004; Sullivan *et al.*, 2001). Biochemically, porcine and human skins have similar collagen matrix and keratinous proteins (Singer and McClain, 2003). Studies have also shown an excellent agreement between pig and human with respect to wound healing responses from growth factors (Sullivan *et al.*, 2001). Despite these benefits, technical difficulties limit the use of pig models for studies of third-degree burns. Indeed, unlike superficial burn wounds, which can easily be created using accessible tools and temperatures, there is limited literature on modeling severe burn injuries in a reproducible manner and on the criteria for assessing the healing kinetics, especially for the purpose of evaluating biomaterials.

Our laboratory has developed an acellular dextran-based hydrogel, dextran-allyl isocyanate-ethylamine, that is tailored to promote rapid neovascularization and has proven to accelerate third-degree burn healing with complete skin regeneration in a murine model (Sun *et al.*, 2010; Sun *et al.*, 2011). The present study tested the efficacy and mechanism by which dextran hydrogel promote regenerative healing in third-degree porcine burn wound model.

Results

Dextran-based hydrogels for third-degree burn wounds in pigs

We generated dextran-based hydrogels modified with allyl isocyanate and ethylamine functional groups and cross-linked with polyethylglycol diacrylate (Sun *et al.*, 2010; Sun *et al.*, 2011). In order to investigate the safety, efficacy action mechanism of the dextran-based hydrogel in the porcine third-degree burn injury model, we designed a custom-made device inspired from a previous study (Branski *et al.*, 2008). This device which is comprised of three parts including metal heat source, and insulation and pressure units (**Figure 1ai**), allows for reproducible delivery of the temperature, the duration of the contact with the object and the pressure.

To create the wounds, the device was held at a 90° angle to the skin with a constant pressure of 2kg/cm^2 (**Fig. 1aii**). As significant thermal insult is associated with progressive injury to deep tissues compared to superficial damages until 48 hours post-injury (Papp *et al.*, 2004), the degree of burn damage was evaluated in wounds 24 hours or 48 hours after the burn (Branski *et al.*, 2008; Gaines *et al.*, 2013). Healthy porcine skin tissue sections are shown in **Supplementary Fig. 1**. To induce full thickness dermal injury, a heat source of 200°C, applied for 30 seconds was required (**Fig. 1b**). In contrast, application of a heat source of 100°C for either 30 or 60 seconds caused injury to the superficial dermis but did not reliably cause full thickness (third-degree) burn injury (**Fig. 1b**; data not shown). As anticipated, evidence of dermal injury progressed between 24 and 48 hours. Thus, use of 200°C for 30 seconds was chosen to generate third-degree burns in assessing the ability of the dextran-based hydrogel to improve healing of burn wounds. The significant damage induced by thermal injury in this model is also evidenced by the reduction in blood flow, indicating more severe damage on blood vessels (**Fig. 1c** and **1d**) and the lack of blood vessels throughout the depth of the injured dermis 48 hours after application of the 200°C for 30 seconds (**Fig. 1e**).

Vascular ingrowth, maturation, and regression in hydrogel-treated burn wounds

Following excision of the necrotic tissue after 48 hours, hydrogels were applied as skin substitutes. Because complete excision of the avascular zone of coagulation has been shown to improve outcomes when biomaterials are used for burn wound treatment, we investigated whether it was necessary for maximal efficacy to resect beyond the original injury site (complete) or whether a more conservative resection (partial) would be sufficient. In the first protocol, we followed the approach used in our previously published murine burn model in which a 1.2 cm diameter biopsy punch was used to excise the burn wound made by a 1.2cm diameter stainless steel device (Sun *et al.*, 2011) and excised the entire initial contact site of the thermal burn. The excised areas were then treated with pre-crosslinked hydrogels shaped to fit the size of the wounds. In the second protocol, all the necrotic tissue was excised, up to 3mm in diameter beyond the initial contact site (**Supplementary Movie 1**).

Immunohistochemical staining for CD31, was seen by day 5 only in wounds that had complete excision of the burn wound. In contrast, incomplete excision negatively impacted vascularization of the hydrogel during that time frame (**Fig. 2a**). Hydrogel vascularization,

quantified both as vessel density and the percentage of area covered by the vessels two weeks post-treatment, confirmed a more efficient vascularization followed by vascular regression for the completely excised wounds, consistent with a superior healing process (**Fig. 2b**), prompting selection of this model for use in all subsequent studies.

We next examined the ability of the hydrogel to promote vascularization and subsequent vessel regression within healing wounds compared to wounds treated with dressing alone following complete excision of burn injured tissue. In the first week after excision, mean vascular density in both groups were increased at both day 5 and 7 when compared to baseline. However, a more rapid vascular regression was noted in hydrogel treated wounds. Specifically, the hydrogel treated wounds exhibited significant decrease in vessel density by day 14, whereas the dressing-only treated group showed no significant change over the same time period (**Fig. 2c**). Blood flow analysis on day 14 confirmed a significant reduction in blood flow in the hydrogel treated wounds compared to dressing-only treated wounds that was closer to that seen in uninjured skin (**Fig. 2d**), supporting hydrogel-induced resolution of the initial vascular phase of wound repair.

Wound closure and re-epithelialization

A key feature of any healed wound is complete reepitheliazation. We have examined dressing versus hydrogel treatment. Occasionally, dressing change interrupted the integrity of the healing area, which prompted us to also examine the re-debridement on day 5 following by re-application of hydrogel or dressing-only. Gross examination of the wounds at day 14 revealed a delay in wound closure in the dressing-only treated wounds compared to hydrogel treated wounds (**Fig. 3ai**).

Examining gross wound closure, we found that all hydrogel treated wounds appeared closed while just 14% of dressing-only treated wounds and none of the dressing retreated wounds were closed (**Fig. 3aii**), resulting in wound gap in the dressing-only treated wounds and larger gap in the dressing retreated wounds (**Fig. 3aiii**). While all hydrogel treated wounds close on day 14, there was a delay in the dressing-only treated wounds. Identification of the neoepithelium on masson trichrome or K14 (keratinocyte marker) stained sections confirmed that dressing-only treated wounds had an epithelial gap, while hydrogel- treated wounds were completely re-epithelialized (**Fig. 3b**). A similar trend was found with retreated wounds where dressing-only retreated wounds had a gap in the epithelial layer while hydrogel retreated wounds were closed with a thick and reticulated epithelial layer (**Fig. 3c**). Correspondingly, dressing-only retreated wounds were only about 50% re-epithelialized compared to hydrogel retreated wounds which were all completely reepithelialized; $p<0.01$. A similar trend was seen for hydrogel single application versus dressing alone control. We next quantified the rete percentage (i.e the percent of the reticulated epithelium in the regenerated epithelium) and the rete ridges (Kiwanuka *et al.*, 2011). We found that dressing-only treated wounds had a very low rete percentage and density, while hydrogel treated and retreated wounds exhibited high rete percentage and rete density. Consistent with a superior regenerative response, hydrogel treated wounds have rete density similar to healthy skin (**Fig. 3di-ii**). Finally, the hydrogel treated and hydrogel retreated wounds exhibited similar decrease in vessel density from day 7 to day 14, whereas

the dressing and dressing re-treated group showed no significant change over the same time period (**Supplementary Fig. 2**). Based on these results, hydrogel treatment (without the retreating) procedure was used to continue our analyses of healing kinetic and remodeling.

Healing kinetics

To further analyze whether the dextran hydrogel treated wounds heal in a more efficient manner, gene array analysis on days 5,7, and 14 post treatment was performed. In general, we found that there was a higher expression of inflammatory mediators at day 5, suggestive of a stronger inflammatory response for dressing-only treated group, compared to hydrogel treated wounds and which regressed as time progress (**Fig. 4a**). Notably, expression analysis suggests a persistence of inflammation may be driven by sustained expression of mediators such as chemokine (CCL2) and tumor necrosis factor (TNF) in the dressing treated wounds compared to hydrogel-treated wounds (**Fig. 4b**). Immunostaining for macrophage marker (MAC387) revealed an abundance of macrophages throughout the granulation tissue at day 5 in the dressing-only treated wounds, which decreased in density on day 7. In contrast, although macrophages were present in dextran hydrogel treated wounds, significantly less macrophages were found in the granulation tissue in both time points (**Fig. 4c**). In the meantime, hydrogel treatment induced expression of ECM and remodeling genes compared to control (dressing only treated) wounds beginning at day 7 with differences maintained through day 14, suggesting superior granulation tissue formation (replacement of the hydrogel with native matrix and fibroblasts) and more efficient remodeling of this matrix in hydrogel-treated wounds (**Fig. 4d**). Overall, these results suggest that hydrogels, in comparison to treatment with dressing only, can promote a controlled healing response that is characteristic of a regenerative response including efficient resolution of inflammation, promotion of an ECM rich granulation tissue with accelerated vascular regression and a superior rate of reepithelialization and quality of neoepithelium formed.

Wound Remodeling and Re-innervation

To further examine the effect of hydrogel treatment on dermal remodeling, we analyzed dermal ECM protein composition at day 40 post treatment. We found that mature collagen fibers could be observed throughout the neodermis of hydrogel treated wounds, while dressing treated wounds had mature collagen fibers primarily at the periphery of the wounds as evidenced by Masson trichrome staining (**Fig. 5a** and **5ci**). Moreover, we found that elastic fibers were present in the periphery of hydrogel-treated wounds but were significantly reduced in dressing treated wounds (**Fig. 5bi-ii, 5cii**), suggesting that hydrogel treated wounds were at a more advanced stage of remodeling compared to dressing treated wounds at the same time.

In addition to significantly increased deposition of collagen and elastin fibers in hydrogel treated wounds compared to controls, gene analysis revealed significant upregulation of KAL1 and Laminin alpha 2 mRNA expression (**Fig. 5d**). These two genes are associated with neuron guidance (Blais *et al.*, 2009; Blais *et al.*, 2013; Tengara *et al.*, 2010) indicating a potential greater peripheral neuron infiltration. Here, neuronal marker protein gene product 9.5 shows that while both wound types have nerve fibers present at the edges of the wounds,

peripheral nerve ingrowth to the central portion of the wounds was observed only in the hydrogel-treated wounds but not in the dressing-treated wounds (**Fig. 5e**).

Discussion

Full- or split-thickness skin grafting is the current gold standard for wound closure following severe burn wound injury. A few synthetic substitutes have made their ways to the market, but most provide only a temporary barrier until autografts are available for permanent closure (Supp, 2011). To the best of our knowledge, there is no synthetic product currently indicated for treating third-degree burns. We began by establishing a reproducible protocol for creating third-degree burn wounds in adult pigs. For third-degree burns in adult pigs, we found that 200°C provides the sufficient heat for the wounds to progress into a full-thickness dermal damage within 48 hours. This progression of burn injury after the initial heat damage is also seen in human burn patients (Nanney *et al.*, 1996).

Therefore, we theorized that treatment methods could impact the healing kinetics. In terms of treating the wounds with the dextran hydrogels, we found that completely excising the necrotic skin accelerated the infiltration of blood vessels into the treated areas and more profound regression of the neovessels over time, indicating better healing kinetics. Comparing dextran-based hydrogel treatment to the dressing-only treated wounds, wound closure was accelerated in dextran-based hydrogel treated wounds, and the healing occurred in a regenerative fashion, characterized by a rapid angiogenic response followed by vascular regression. Truly, angiogenesis followed by vessel regression plays a crucial role in wound healing progress (DiPietro, 2013; Hanjaya-Putra *et al.*, 2013), but compared to excisional wounds, severe burn wounds exhibit impaired and slower neovascularization, potentially due to delayed mobilization of circulating angiogenic cells (Guo *et al.*, 2014; Hanjaya-Putra *et al.*, 2013; Zhang *et al.*, 2010). Furthermore, rapid re-epithelialization and high quality of epithelium formed were present in the dextran-based hydrogel treated wounds compared to control wounds. Even when the healing process was interfered with debridement, additional topical treatment with the hydrogel allowed fast re-epithelialization, demonstrating the robustness of the hydrogel treatment and its potential in the clinics. The rapid wound closure in the dextran treated burns may be due to combination of factors including the moist environment provided by the hydrogels, which leads to a more efficient re-epithelialization and faster stromal cell migration (Boateng *et al.*, 2008), excellent mechanical properties along with charged functional groups of the dextran hydrogel (Sun *et al.*, 2010), and the high angiogenic capability of the dextran hydrogel (Sun *et al.*, 2010; Sun *et al.*, 2011) result in an overall quicker and better epidermis reconstruction.

The rapid onset and regression of the inflammatory response plays a crucial role in coordinating the process of wound healing (Gurtner *et al.*, 2008). We found higher expression of proinflammatory mediators on day 5 in the dressing treated wounds compared to the hydrogel treated wounds suggesting persistent inflammatory response. While the necessity of inflammatory response in wound healing is debated (Ashcroft *et al.*, 1999; Martin *et al.*, 2003), in the context of biomaterial-induced healing, appropriate timings and durations of acute and chronic inflammatory responses would be needed for better healing results (Koh and DiPietro, 2011). Gene array analysis revealed lesser inflammatory response

in the hydrogel treated group than in the dressing-only treated group. Immunohistochemistry showed high density of macrophages in the dressing treated wounds on day 5, which regressed by day 7. In contrast, only few macrophages in the dextran hydrogel treated wounds could be observed during these time points. Since inflammatory cells, especially macrophages, secrete essential cytokines and growth factors necessary for angiogenesis and stromal cell migration (Eming *et al.*, 2007), the elevated neovascularization followed by early vascular regression in the hydrogel treated group strongly suggests earlier onset of the inflammatory response.

During wound remodeling stage, the granulation tissue is being remodeled in order to reconstruct the loose regenerated dermis and strengthen the repaired tissue (Gurtner *et al.*, 2008). The severity of scarring depends on the amount and the organization of the secreted ECM during this phase. Therefore, an ideal skin substitute would induce high ECM deposition and organized crosslinking of ECM fibers in order to minimize scarring. Gene array analysis indicated that hydrogel treatment induced the expression of ECM and remodeling genes on days 7 and 14. Indeed, after 40 days of treatment, hydrogel treated healing wounds showed higher density of collagen compared to the dressing-only group, and the structure of the newly deposited collagen observed in the hydrogel treated wounds showed higher organization. In addition, elastin fibers, which is usually poorly restored in scars (Lamme *et al.*, 1996), were deposited in higher density in hydrogel treated wounds. Together with collagen, the regeneration of elastin provides favorable fiber frameworks for the later phase of wound healing (Eming *et al.*, 2007).

Since the skin is also a highly sensitive organ, after a deep burn injury, cutaneous nerves regenerates from the wound bed with the new nerve fiber migration, or collateral sprouting from the adjacent skin (Blais *et al.*, 2013). In fact, burn victims often suffer permanent sensory deficits from abnormal sensation to chronic pain (Malenfant *et al.*, 1996; Ward *et al.*, 1989; Ward and Tuckett, 1991). As a result, neuron regeneration poses a major challenges in order to improved patients' quality of life by restoring its sensory perceptions of the regenerated skin. We found that dextran hydrogel treatment promoted nerve ingrowth into the regenerated skin with the nerve fibers presents close to the center of the wound on day 40. In contrast, we were unable to locate nerve fiber in the dressing treated wounds. Combining our findings, the hydrogel treatment not only induced ECM remolding, but also improved the re-innervation of the repaired wound. Further examination of the nerve fiber will be need to identify which type and maturity of nerve fibers as well as the mechanism of the recruitment. While we examined our samples, we found that these nerve fibers often time co-localized with the blood vessels. We thus speculate that perhaps the enhanced neovascularization during hydrogel treatment as well as more rapid re-epithelialization consequently contributed greater neural ingrowths during the healing progress.

It is important to note that the treatment groups utilized in our study are modeled on clinical care guidelines for third-degree burn wounds. Although the burn wound is completely excised in this model prior to hydrogel application, these wounds cannot be considered simple excisional wounds. Locally, edema develops even beyond the periphery of the excised tissue (as shown in Figure 1c). In addition, this model likely also captures the systemic hypermetabolic response which is characteristic of third-degree burn injury that

includes hyper-inflammation, hormonal dysfunction and catabolism (Jeschke *et al.*, 2007; Orgill, 2009; Williams *et al.*, 2009), although these parameters were not specifically examined in the current study. As such, these wounds differ from simple excisional wounds for local tumor removal or acute localized trauma. Given this systemic response to burn injury and the delay in excision, comparison of these wounds to simple excisional wounds in the same individual pig is invalid. Although the current study does not compare healing between this model and simple excisional wounds, future studies will explore the use of our hydrogels for other types of wounds including acute injury models. Finally, whether the dextran-based hydrogel supports better healing than other commercially available hydrogels was not examined in this study.

Our study establishes a robust protocol for injury and hydrogel treatment of third-degree burns in a porcine large-animal model and thus paves the way for their use in clinical studies. The specific model was developed based on the surgical excision and grafting of full-thickness burn wounds that has been common clinical practice for over 60 years (Cope *et al.*, 1947) and reflects current clinical guidelines (Jeschke *et al.*, 2013). Encouragingly, treating burned, full-thickness wounds with our dextran-based hydrogel allows functional regeneration of the tissue through fast neovascularization and epithelial wound closure. In addition, the dextran hydrogel promotes more efficient dermis reconstruction and enhanced re-innervation. Overall, our findings support dextran-based hydrogels as an ideal candidate of next generation of low-cost, off-the-shelf and readily available treatment of a range of dermal injuries, which may enhance wound care for patients when skin autograft is neither available nor desirable.

Materials and Methods

Hydrogel Treatment and Surgical Procedure

The dextran hydrogel was synthesized and characterized as previously (Sun *et al.*, 2010; Sun *et al.*, 2011). *In vitro* cell toxicity was carried out using WST assay (Sigma) and pilot *in vivo* mice tests (Sun *et al.*, 2011) to confirm the dextran hydrogel therapeutic properties.

Surgical procedures were approved by the Institutional Animal Care and Use Committee at Thomas D. Morris, Inc. prior to the experiments. Two pigs were used to determine optimal wounding procedure and parameters for third degree burn. Temperature was set at 100°C and 200°C while maintaining contact pressure at 2kg/cm^2 and contact duration of 30 seconds. Biopsy was taken 24 and 48 hours after injury for histological analysis. Three pigs were then used to investigate the therapeutic effect of dextran hydrogel on burn wounds. Following injury, the wounds were left for 48 hours for stabilization before the excision procedure. A total of 70 circular third-degree burn wounds (1.2 or 1.5cm in diameter) were created. Circular biopsy punches were used for partial or complete excision for full-thickness wound down to the necrotic adipose layer. Wounds were at least 3cm apart from one another to minimize hindered wound healing process due to proximity. After the excision procedure, wounds were cleaned with sterile gauze to temporarily stop bleeding. Half of the wounds were treated with dextran hydrogel and the other half were left untreated. Treated and untreated wounds were first sealed with Tegaderm® (3M) and compound benzoin tincture (Medical Chemical, Corp) to enhance the Tegaderm® adherence

to the skin. An additional layer of Vetrap® (3M) and elastic body suit (VetMedCare) were worn over the body. To protect the newly forming epidermis from traumatization during bandage change, a non-adhesive Curity® dressing (Covidian) was placed under the Tegaderm® layer. After wound closure, only an elastic body suit was worn over the wounds. For retreatment, re-debridement was made and a new half the thickness hydrogel was placed on top for retreatment. Secondary excision was made on control group as well for the retreatment group. Dressings were changed three times a week until wound closure was complete. This dressing procedure as well as maintenance conditions were consistent between pigs throughout the duration of the experiments.

Healing Evaluation

Blood flow was monitored noninvasively using moorFLPI speckle contrast imager (Moor Instruments, Inc.). The measurements were normalized by the blood flow measurements of the healthy skin area adjacent to each wound.

For immunohistochemical assay, collected skin specimens were fixed, embedded in paraffin. Bisected wounds were sectioned serially to ensure analysis of the mid-point of the wounds, as previously (Swift *et al.*, 2001). Histologic sections were stained with Haematoxylin and Eosin (H&E), Masson trichrome, and Verhoeff-van Gieson's stain or immunohistochemistry for CD31, cytokeratin 14, MAC387 (all from abcam), SMA (Dako), Dapi, PGP9.5 (AbD Serotec) and matching Alexaflour secondary (Lifetech). Histological images were taken with upright light microscope and Camera (Nikon). Full specimens images were scanned using automated motor controlled Nikon T1 and tiled together with corresponded software (Nikon Nis-Element). Fluorescent images were taken with confocal (Zeiss LSM780). The area and number of vessels inside the wounds were quantified from CD31 stained sections using ImageJ software (National Institutes of Health) as previously (Hanjaya-Putra *et al.*, 2013; Sun *et al.*, 2011). Wound gap area was measure photometrically. Re-epithelialization was calculated as the percentage of regenerated epithelium (K14 positive) of the entire wound. Maturation of the re-epithelialization was quantified by rete ridge formation density as previously described (Kiwanuka *et al.*, 2011). Collagen fiber deposition was quantified from Masson trichrome images by calculating the percentage of collagen fiber presented in the wound. Using ImageJ, we quantified the percentage of stained collagen fibers in the given area in each group. Elastin fibers were quantified from Verhoeff-van Gieson's stain across the dermis area adjacent to the epidermis similarly to the collagen. Nerve innervation analysis was performed on a 25μm paraffin sections on gelatin-coated slides. Slides were then analyzed in confocal using serial z-stack imaging.

Gene expression analysis was performed using two-step reverse transcription polymerase chain reaction (RT-PCR) on wound specimens in accordance with Applied Biosystems manufacturer instructions. Wound healing and ECM RT-PCR array sets (Qiagen) were used to compare the expression profile. For each primer, the comparative computerized method provided by the manufacturer was used to calculate the amplification differences between different samples.

Statistical Analysis

For wounding parameter determination two pigs were used. For wound healing analysis, total of three pigs with n>12 wounds for each condition with at least n=3 for each time point detailed throughout the manuscript. For quantification of blood vessels and reepithelialization whole wounds analyzed as detailed above. Real-time RT-PCR performed on triplicate samples (n=3) with triplicate readings. Statistic was calculated by the computerized method provided by the manufacturer to obtain p-value of the gene expression. For data presentation relative gene expression was graphed with relative fold change of the targeted group / dressing day 5. For all other assays, statistical analysis was performed using GraphPad Prism 6.01 (GraphPad Software Inc.) to perform t-tests, One Way ANOVA with Turkey's posttest, or Two Way ANOVA with Bonferroni's posttest where appropriate. Significance levels were set at *p<0.05, **p<0.01, ***p<0.001, and ****p<0.0001. Unless otherwise indicated, all graphical data are reported ±SD.

Supplementary Material

Refer to Web version on PubMed Central for supplementary material.

Acknowledgments

We thank Markus Tammia and Dr. Hai-Quan Mao for assistance with neuronal stain. This work was supported by Gemstone Biotherapeutics LLC and NIH grant R01HL107938 (to S.G).

References

Ashcroft GS, Yang X, Glick AB, et al. Mice lacking Smad3 show accelerated wound healing and an impaired local inflammatory response. Nature cell biology. 1999; 1:260–6. [PubMed: 10559937]

Blais M, Grenier M, Berthod F. Improvement of nerve regeneration in tissue-engineered skin enriched with schwann cells. The Journal of investigative dermatology. 2009; 129:2895–900. [PubMed: 19587695]

Blais M, Parenteau-Bareil R, Cadau S, et al. Concise review: tissue-engineered skin and nerve regeneration in burn treatment. Stem cells translational medicine. 2013; 2:545–51. [PubMed: 23734060]

Boateng JS, Matthews KH, Stevens HN, et al. Wound healing dressings and drug delivery systems: a review. Journal of pharmaceutical sciences. 2008; 97:2892–923. [PubMed: 17963217]

Branski LK, Mittermayr R, Herndon DN, et al. A porcine model of full-thickness burn, excision and skin autografting. Burns : journal of the International Society for Burn Injuries. 2008; 34:1119–27. [PubMed: 18617332]

Cope O, Langohr JL, Moore FD, et al. Expeditious care of full-thickness burn wounds by surgical excision and grafting. Annals of surgery. 1947; 125:1.

DiPietro LA. Angiogenesis and scar formation in healing wounds. Current opinion in rheumatology. 2013; 25:87–91. [PubMed: 23114588]

Eming SA, Krieg T, Davidson JM. Inflammation in wound repair: molecular and cellular mechanisms. The Journal of investigative dermatology. 2007; 127:514–25. [PubMed: 17299434]

Gaines C, Poranki D, Du W, et al. Development of a porcine deep partial thickness burn model. Burns : journal of the International Society for Burn Injuries. 2013; 39:311–9. [PubMed: 22981797]

Guo R, Teng J, Xu S, et al. Comparison studies of the in vivo treatment of full - thickness excisional wounds and burns by an artificial bilayer dermal equivalent and J - 1 acellular dermal matrix. Wound Repair and Regeneration. 2014; 22:390–8. [PubMed: 24844338]

Gurtner GC, Werner S, Barrandon Y, et al. Wound repair and regeneration. Nature. 2008; 453:314–21. [PubMed: 18480812]

Hanjaya-Putra D, Shen Y-I, Wilson A, et al. Integration and Regression of Implanted Engineered Human Vascular Networks During Deep Wound Healing. Stem cells translational medicine. 2013; 2:297–306. [PubMed: 23486832]

Hop MJ, Polinder S, van der Vlies CH, et al. Costs of burn care: A systematic review. Wound repair and regeneration : official publication of the Wound Healing Society [and] the European Tissue Repair Society. 2014; 22:436–50.

Jeschke MG, Finnerty CC, Suman OE, et al. The effect of oxandrolone on the endocrinologic, inflammatory, and hypermetabolic responses during the acute phase postburn. Annals of surgery. 2007; 246:351–60. discussion 60-2. [PubMed: 17717439]

Jeschke, MG.; Kamolz, L.; Shahrokhi, S. Burn Care and Treatment: A Practical Guide. Springer Vienna; Vienna: 2013.

Kiwanuka E, Hackl F, Philip J, et al. Comparison of healing parameters in porcine full-thickness wounds transplanted with skin micrografts, split-thickness skin grafts, and cultured keratinocytes. Journal of the American College of Surgeons. 2011; 213:728–35. [PubMed: 22018809]

Koh TJ, DiPietro LA. Inflammation and wound healing: the role of the macrophage. Expert reviews in molecular medicine. 2011; 13:e23. [PubMed: 21740602]

Lamme EN, de Vries HJ, van Veen H, et al. Extracellular matrix characterization during healing of full-thickness wounds treated with a collagen/elastin dermal substitute shows improved skin regeneration in pigs. Journal of Histochemistry & Cytochemistry. 1996; 44:1311–22. [PubMed: 8918906]

Malenfant A, Forget R, Papillon J, et al. Prevalence and characteristics of chronic sensory problems in burn patients. Pain. 1996; 67:493–500. [PubMed: 8951946]

Martin P, D'Souza D, Martin J, et al. Wound healing in the PU.1 null mouse--tissue repair is not dependent on inflammatory cells. Current biology : CB. 2003; 13:1122–8. [PubMed: 12842011]

Middelkoop E, van den Bogaerdt AJ, Lamme EN, et al. Porcine wound models for skin substitution and burn treatment. Biomaterials. 2004; 25:1559–67. [PubMed: 14697858]

Nanney LB, Wenczak BA, Lynch JB. Progressive burn injury documented with vimentin immunostaining. Journal of Burn Care & Research. 1996; 17:191–8.

Orgill DP. Excision and Skin Grafting of Thermal Burns. New England Journal of Medicine. 2009; 360:893–901. [PubMed: 19246361]

Papp A, Kiraly K, Härmä M, et al. The progression of burn depth in experimental burns: a histological and methodological study. Burns : journal of the International Society for Burn Injuries. 2004; 30:684–90. [PubMed: 15475143]

Sheridan, RL. Burns : a practical approach to immediate treatment and long-term care. Manson Publishing; London: 2012.

Singer AJ, McClain SA. A Porcine Burn Model. Wound Healing: Methods and Protocols. 2003; 78:107–19.

Stoddard FJ Jr. Ryan CM, Schneider JC. Physical and Psychiatric Recovery from Burns. The Surgical clinics of North America. 2014; 94:863–78. [PubMed: 25085093]

Sullivan TP, Eaglstein WH, Davis SC, et al. The pig as a model for human wound healing. Wound repair and regeneration. 2001; 9:66–76. [PubMed: 11350644]

Sun G, Shen YI, Ho CC, et al. Functional groups affect physical and biological properties of dextran-based hydrogels. Journal of biomedical materials research Part A. 2010; 93:1080–90. [PubMed: 19753626]

Sun G, Zhang X, Shen YI, et al. Dextran hydrogel scaffolds enhance angiogenic responses and promote complete skin regeneration during burn wound healing. Proceedings of the National Academy of Sciences of the United States of America. 2011; 108:20976–81. [PubMed: 22171002]

Supp DM. Skin substitutes for burn wound healing: current and future approaches. 2011

Swift ME, Burns AL, Gray KL, et al. Age-related alterations in the inflammatory response to dermal injury. The Journal of investigative dermatology. 2001; 117:1027–35. [PubMed: 11710909]

Tengara S, Tominaga M, Kamo A, et al. Keratinocyte-derived anosmin-1, an extracellular glycoprotein encoded by the X-linked Kallmann syndrome gene, is involved in modulation of epidermal nerve density in atopic dermatitis. Journal of dermatological science. 2010; 58:64–71. [PubMed: 20219326]

Ward RS, Saffle JR, Schnebly WA, et al. Sensory loss over grafted areas in patients with burns. The Journal of burn care & rehabilitation. 1989; 10:536–8. [PubMed: 2600103]

Ward RS, Tuckett RP. Quantitative threshold changes in cutaneous sensation of patients with burns. The Journal of burn care & rehabilitation. 1991; 12:569–75. [PubMed: 1779012]

Williams FN, Jeschke MG, Chinkes DL, et al. Modulation of the hypermetabolic response to trauma: temperature, nutrition, and drugs. J Am Coll Surg. 2009; 208:489–502. [PubMed: 19476781]

Zhang X, Wei X, Liu L, et al. Association of increasing burn severity in mice with delayed mobilization of circulating angiogenic cells. Archives of Surgery. 2010; 145:259–66. [PubMed: 20231626]

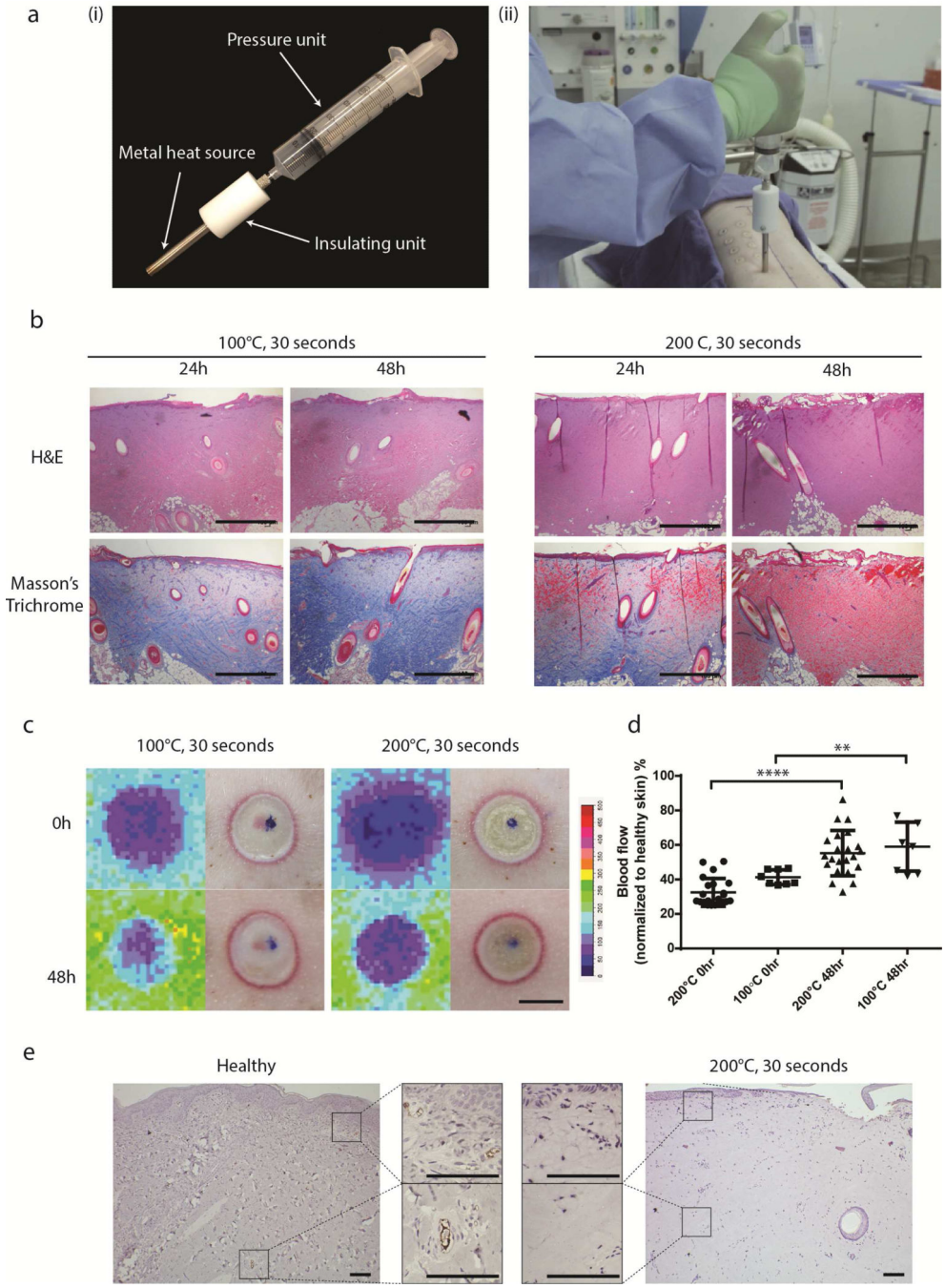

Figure 1. Induction of third degree burn injury in pigs

(**a**) A custom-made burn device (i) is held upright on the pig's thoracic paravertebral zone (ii). (**b**) Representative images of H&E and mason trichrome histological stains of the wounds at different temperatures and burn durations. (**c-d**) Laser speckle contrast images (*left*) and quantification (*right*) of blood flow in healthy skin and burn wounds burn wound. N= 22 and N=8 for 200°C and 100°C respectively. (**e**) Immunohistochemistry for CD31 of the 200°C 30 seconds 48h show no vessels in the wounded area compared to healthy skin.

Significance levels were set at *p<0.05, **p<0.01, ***p<0.001, and ****p<0.0001.Scale bars are 1mm in **b**, 1cm in **c** and 100μm in **e**.

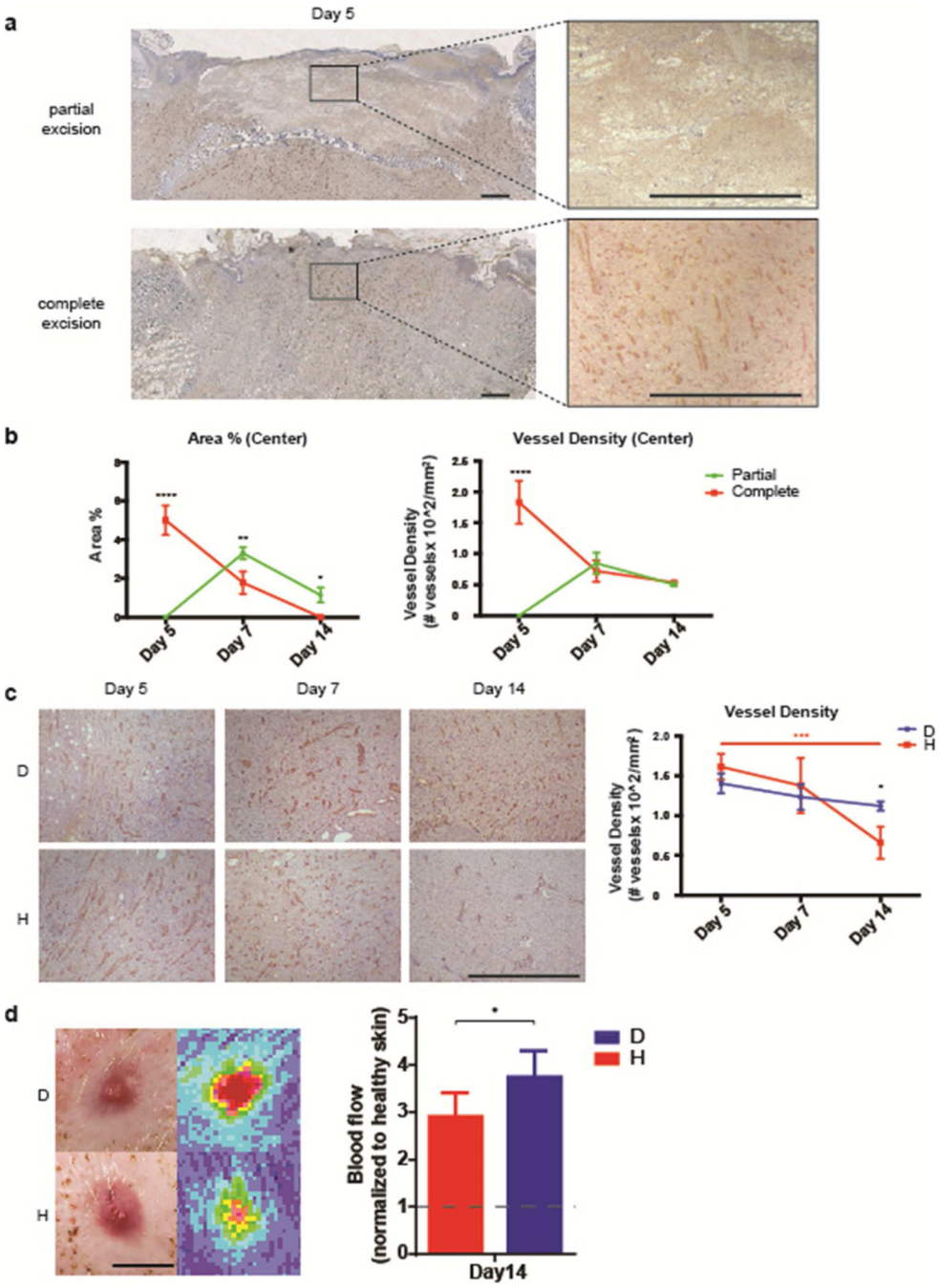

Figure 2. Wound excitement and kinetics of vascularization

(**a**) Immunohistochemistry for CD31 of wound area depicting vascular ingrowth on day 5 for partially excised (method 1) and completely excised (method 2). High magnifications of the boxed areas are shown on the right. (**b**) Quantification of CD31 stains at of the wounds treated in both methods over two weeks N=3 per time point. (**c**) CD31 and quantification of vasculature over two week of the wounds.N=3 per time point. (**d**) Laser speckle contrast images (right) and quantification (left) of blood flow on day 14. D= dressing-only treated wounds; H= hydrogel treated wounds. N=7. Scale bars are 1mm in **a** and **c** and 1cm in **d**.

Red asterisks indicate significant change along time; Black asterisk indicate significant difference between the two treatments at a given time point. Significance levels were set at *p<0.05, **p<0.01, ***p<0.001, and ****p<0.0001.

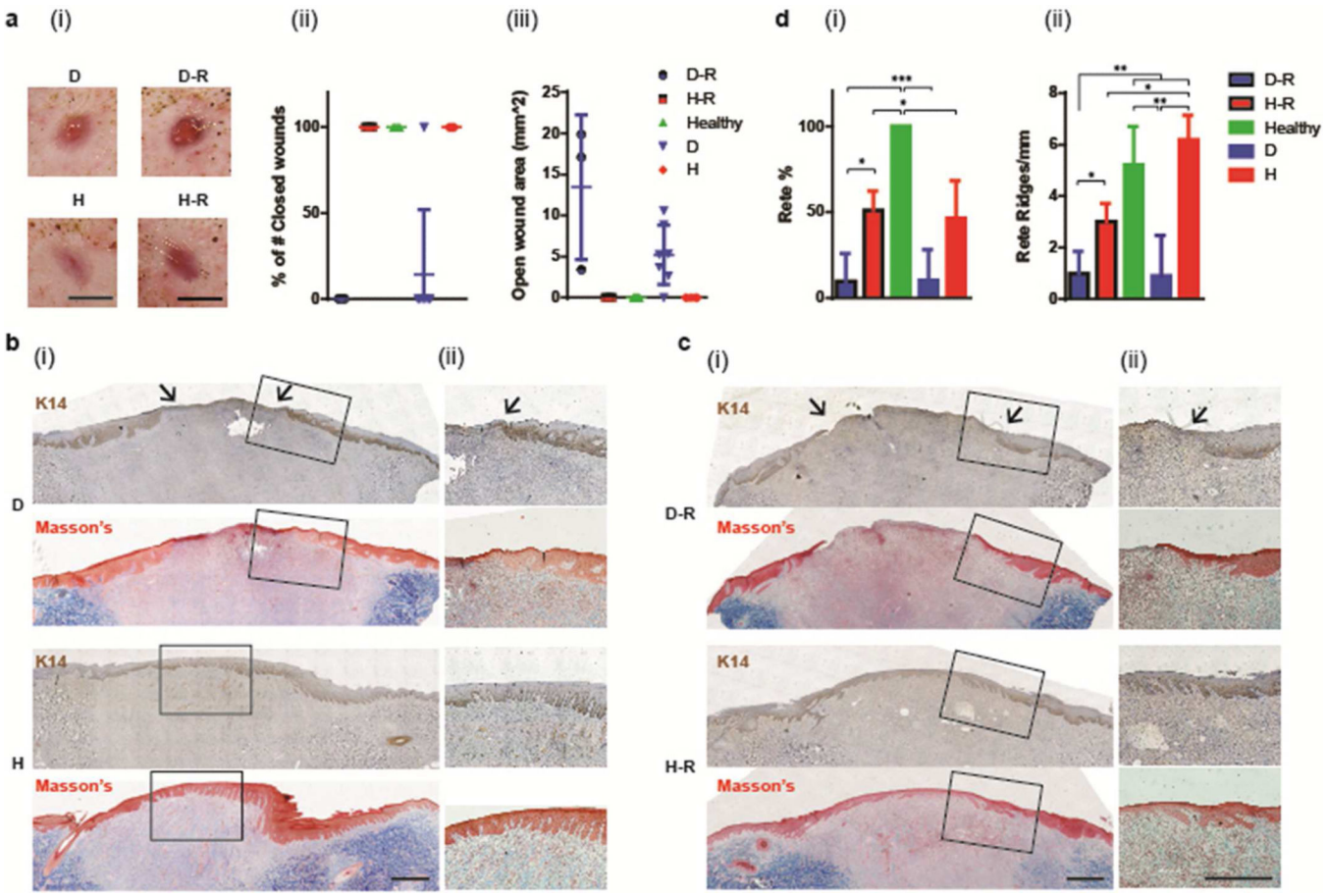

Figure 3. Wound closure and re-epithelialization

(**a**) Wounds on day 14: (i) representative wound images; (ii) percentage closed wounds gap and (iii) open wound area. D= dressing-only treated wounds; H= hydrogel treated wounds; D-R= dressing retreated wounds; H-R= hydrogel retreated wounds. N=7 for D and H and N=3 for D-R and H-R. (**b, c**) Wounds on day 14: (i) representative wound images and (ii) immunohistochemistry for K14 (upper panel; arrows indicate open wound) and masson trichrome stain (lower panel). High magnifications of the boxed areas are shown on the right.; (**c**) Wounds on day 14: (**d**) Quantification of (i) rete percentage and (ii) rete density of day 14-treated wound. N=3. Scale bars are 1cm in **a**i and **b**i; 1mm in **a**ii, **b**ii and 0.5mm in high magnification inserts. Significance levels were set at *p<0.05, **p<0.01, and ***p<0.001.

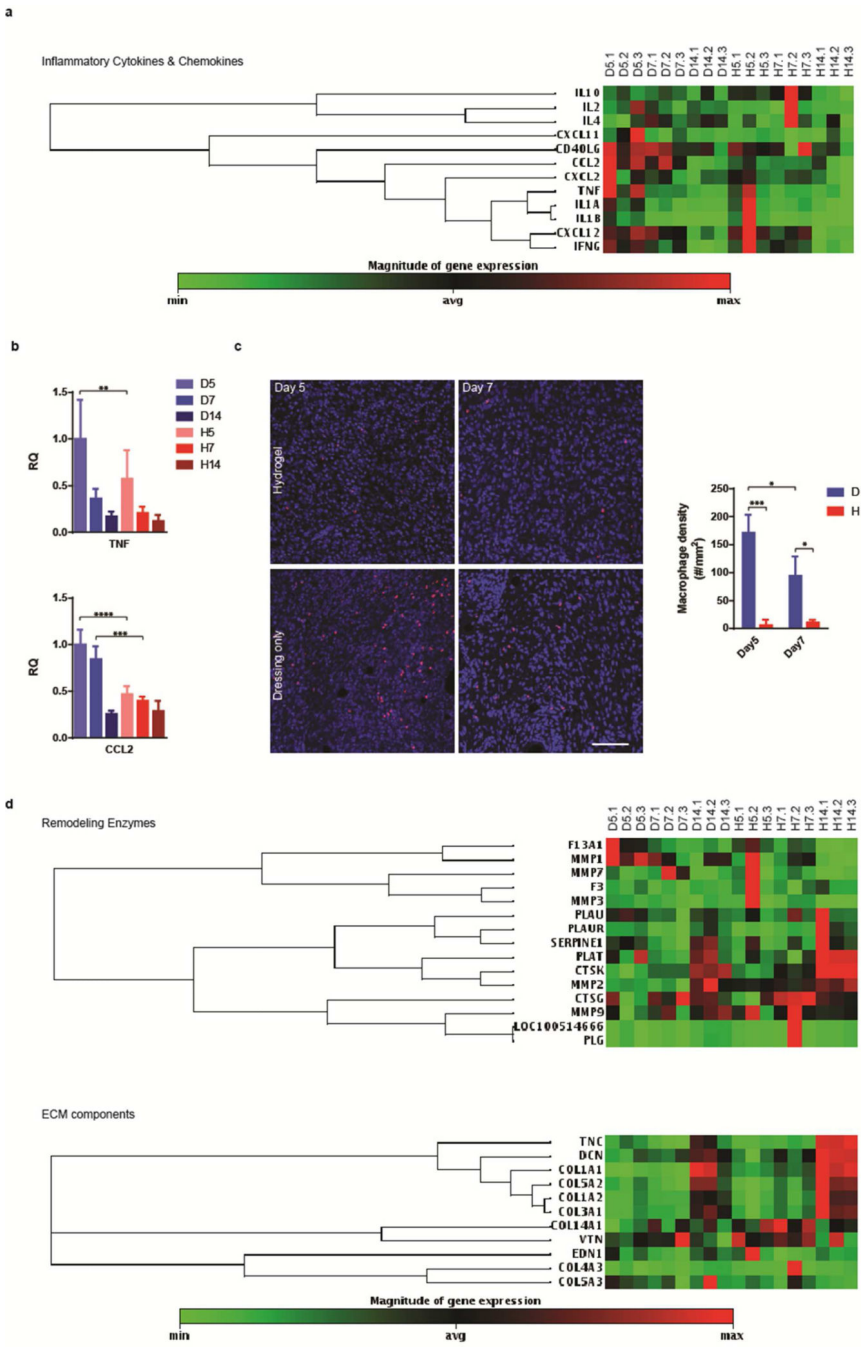

Figure 4. Healing kinetics

(**a**) Wound healing gene array analysis for inflammatory mediators on day 5,7 and 14. (**b**) Relative gene expression of TNF and CCL2 of the treatments on day 5,7 and 14. (**c**) (*left panel*) Representative images of immunefluorescence stain for macrophage (red; nuclei in blue) and (*right panel)* quantification of macrophage density in the wound area on days 5 and 7. (**d**) Wound healing gene array analysis for ECM associated genes on day 5,7 and 14. D= dressing-only treated wounds; H= hydrogel treated wounds. Significance levels were set at *p<0.05, **p<0.01, and ***p<0.001

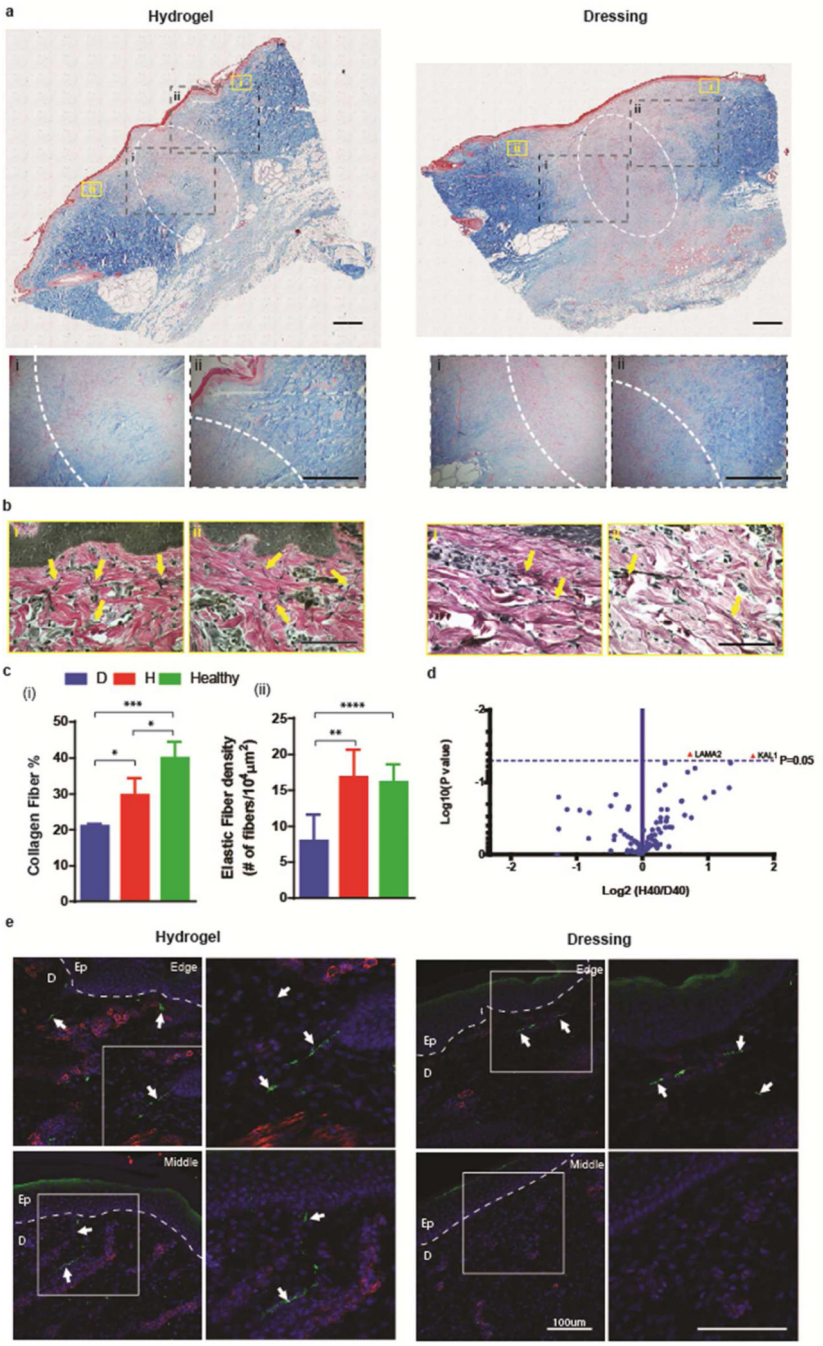

Figure 5. Remodeling and reinnervation of third-degree burns

(**a**) Masson Trichome of d40. High magnifications of the boxed areas. (**c**) (i) Quantification of collagen fiber % in the wounded area (indicated in the white dotted circle in A). (ii) Quantification of elastin fiber density in the dermis area adjacent to the epidermis. N=4 (**b**) Representative images of Verhoeff–Van Gieson. With high magnification insert. Yellow arrows indicate mature elastin fibers. (**d**) Gene array analysis for wound remodeling. **(e)** Neuronal fibers (indicated by white arrows) at the edge of the wounds and in the middle of dressing-only treated (right panel) and hydrogel-treated (left panel) treated wounds. Neurons

(PGP9.5) in green, blood vessels (SMA) in red, nuclei (Dapi) in blue). Scale bars are 1mm in **a** and 100μm in **c and e**. Significance levels were set at *p<0.05, **p<0.01, and ***p<0.001